JOURNAL OF PROPULSION AND POWER
Vol. 22, No. 1, January–February 2006

# Heat-Recirculating Combustor Using Porous Inert Media for Mesoscale Applications

T. L. Marbach*
*University of Oklahoma, Norman, Oklahoma 73072*
and
A. K. Agrawal†
*University of Alabama, Tuscaloosa, Alabama 35406*

**Small-scale power-generation systems offer an alternative to traditional batteries because of the high-energy density of hydrocarbon fuels. Combustion at small scales presents several challenges, including high heat loss and short flow residence times. Heat recirculation is an effective method to limit heat loss and improve combustion performance. However, new methods of achieving heat recirculation in a small volume must be developed for practical devices. To meet this requirement, a heat-recirculating, lean premixed combustion system using porous inert media (PIM) in the combustion chamber and in the preheating annulus around the combustor has been developed. System performance for a range of operating conditions was determined experimentally using methane fuel. Measurements include preheat and product gas temperatures and emissions of CO and NOx. Results show that the reactants were preheated in excess of 600 K by recirculating thermal energy from the reaction zone. Heat loss to the surroundings decreased and heat recirculation to the reactants increased with PIM in the annulus and with insulation of exterior surfaces of the system.**

## I. Introduction

THE need for advanced small-scale combustion systems has arisen in the last decade to develop an alternative to traditional batteries for energy storage.[1,2] With the miniaturization of microelectromechanical devices and personal electronics, the power sources have become a larger fraction of the size and weight of the overall system. Micro- and mesoscale power-generation systems provide a potential solution to this problem because the energy storage density of hydrocarbon fuels is roughly 100 times that of modern batteries. Microthrusters and microrockets are other applications requiring advanced small-scale combustion systems.

With regard to small-scale combustion systems, no universal definitions of mesoscale and microscale exist. We consider the term mesoscale to signify combustor diameter from a few millimeters to about one centimeter. The term microscale indicates that the combustor diameter is smaller than the quenching diameter of the given fuel. Much of the early and current research on small-scale power generation has focused on the microscale.[3–5] However, mesoscale combustion has received increasing attention in recent years because of many potential applications.[6–8] For example, a mesoscale power-generation system could supply electrical power for personal electronics. Mesoscale combustors can power small thrusters or rockets. Mesoscale combustion is also useful for gaining insight into combustion phenomena at moderate scales as a step toward developing high-power density, microscale systems.[7]

In a combustion system, heat is generated volumetrically and it is lost to the surroundings through the surface. Thus, miniaturizing a combustor increases the fraction of heat loss to the surroundings compared to that generated within the combustor. Increased fractional heat loss has negative effects on combustion performance, including poor combustion efficiency and flame quenching.[9,10] Another challenge facing combustor miniaturization is the shorter residence time, limiting fuel/air premixing upstream of the reaction zone. Inadequate flow residence time in the combustion zone may lead to incomplete combustion, low combustion efficiency and high pollutant emissions.[1]

Heat recirculation is one method that can be utilized to improve performance of lean premixed combustion.[11] With heat recirculation, the reactants are preheated using thermal energy from the reaction zone. Thus, the flame temperature is higher than the adiabatic flame temperature of the reactants at inlet conditions. Recently, Ahn et al.[12] and Ronney[13] have applied this concept to achieve combustion in a microscale Swiss roll configuration. The reactants and products were brought into proximity in separate spiraling passages upstream and downstream of the reaction zone. Combustion was achieved over a wide range of flow velocities and equivalence ratios using gas phase and catalytic combustion. Ahn et al. and Ronney have shown that heat recirculation is a viable method of achieving and sustaining combustion in small volumes. Swiss roll combustor use a relatively small combustion volume compared to the total volume of the system. However, practical devices require a combustion system that effectively preheats reactants in a smaller volume. Such devices must use high-density liquid fuels that can be prevaporized using heat recirculation.[14,15]

Porous inert media (PIM) combustion is another method of recirculating flame energy to achieve the excess enthalpy combustion.[16] Specifically, the flame is stabilized either on the surface or inside the PIM. In either case, the reactants are preheated by thermal energy conducted and/or radiated from the reaction zone. Combustion performance using PIM at traditional scales has been characterized and reviewed.[17,18] Marbach and Agrawal[19] used silicon–carbide- (SiC-) coated carbon foam as PIM. For identical conditions, combustion inside PIM extended the lean blowoff (LBO) limit compared to combustion on the PIM surface. Marbach and Agrawal[20] showed that PIM improved fuel prevaporization and premixing with air for liquid fuel applications.

We have developed a combustor concept using PIM to recover energy transferred through the combustor wall to preheat reactants. A schematic of the combustor design is presented in Fig. 1. Fuel and air are injected into a PIM-filled annulus surrounding the combustion chamber. The reactants are premixed and preheated in the

Received 10 November 2004; presented as Paper 2005-942 at the AIAA 43rd Aerospace Science Meeting and Exhibit, Reno, NV, 10–13 January 2005; revision received 22 May 2005; accepted for publication 16 June 2005. 

*Assistant Professor, Department of Mechanical Engineering; currently at Sacramento State University, Sacramento, California 95819. Member AIAA.
†Professor, Department of Mechanical Engineering. Senior Member AIAA.

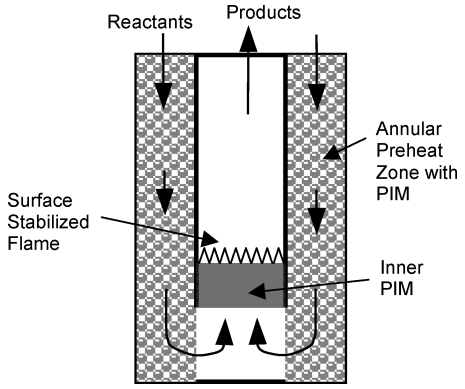


**Fig. 1 Heat-recirculating combustor concept using porous inert media.**

annulus before reaching the inner PIM, which provides additional preheating and premixing of reactants before combustion. The flame is stabilized on the downstream surface of PIM within the combustion chamber. Hot products passing through the combustor chamber transfer heat to the cooler reactants flowing through the annulus. The high surface area of PIM in the annulus is expected to increase interfacial convection in a smaller volume.

The proposed heat-recirculating PIM combustor design has similarities and important differences from similar other designs. Yuasa et al.[3] introduced the concept of a flat flame burner using stainless steel porous plate for microflame applications. In our design, combustion is stabilized on the surface of SiC-coated carbon foam used as PIM. Unlike Yuasa et al., an annular preheat zone is used to reduce heat loss and improve flame stability by preheating the reactants. The Swiss roll combustor design used by Ahn et al.[12] and Ronney[13] improved flame stability by heat recirculation. However, the combustion volume was small compared to the total volume of the system. Our design uses a single-pass annulus filled with PIM to promote heat transfer, instead of multiple passages that increase the overall system size.

## II. Objectives

The objective of this study is to evaluate performance of the heat-recirculating combustor design presented in the Introduction. The combustion performance is quantified by measuring preheat and product gas temperatures and emission of nitric oxides (NOx) and carbon monoxide (CO). Measurements were taken with and without PIM in the annulus and with and without insulation on the exterior surfaces. The operating parameters include mean reactant velocity and equivalence ratio. The overall goal is to assess the feasibility of the proposed design in reducing heat loss to the surroundings and maximizing heat recirculation to preheat the reactants. A larger volume was used in this first-generation system expected to guide future designs of meso- and microscale combustion systems.

## III. Experimental Setup

Figure 2 shows a schematic of the heat-recirculating combustor constructed to perform the experiments. The system size was selected to determine important characteristics of this new design at a moderate scale. Thus, factors such as the ease of manufacturing and instrumentation for detailed measurements were considered. Radial dimensions were chosen to maintain nearly a constant cross-sectional area in the annulus and combustion chamber. The major components were machined from 304 stainless steel. Methane fuel and air were injected separately into the annulus at six equally spaced injection ports. The annulus measured 100 mm long with an inner diameter of 27 mm and an outer diameter of 34 mm. The annulus was filled with an 80-mm-long bed of packed 304 stainless steel spheres of 3 mm diameter. The preheated fuel/air mixture entered the inner passage through four 12-mm-diam peripheral holes. Combustion was stabilized on the downstream surface of the 25-mm-long inner PIM, a monolithic SiC-coated, carbon foam of 12 pores/cm. The free space of the combustion chamber was 20 mm

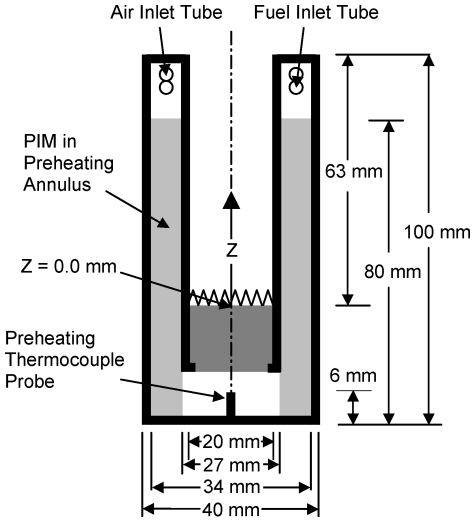


**Fig. 2 Schematic of heat-recirculating combustor used for experiments.**

in diameter and 63 mm long. The combustor was insulated with 25-mm-thick Insulfrax insulation, with thermal conductivity of 0.2 W/m · K (Ref. 21).

Methane fuel was supplied from a compressed gas cylinder and measured with a mass flowmeter calibrated in the range 0–1.0 standard 1/min with an uncertainty of ±0.015 standard 1/min. Air was supplied by an air compressor, dried and measured with a mass flowmeter calibrated in the range 0–60 standard 1/min with an uncertainty of ±1.2 standard 1/min. The preheat temperature was measured by a K-type thermocouple located upstream of the inner PIM, as shown in Fig. 2. The product gas temperature was measured by an R-type thermocouple with 0.075-mm bead diameter. The product gas temperature is reported uncorrected for radiation, and the maximum radiation correction is estimated to be 60 K. The total uncertainty of the temperature measurements was 20 K. Concentrations of NOx and CO were measured with electrochemical gas analyzers calibrated in the range 0–200 ppm with an uncertainty of ±4 ppm. Emissions samples were obtained through a quartz probe of 3 mm outer diameter with a tapered tip of 4:1 expansion ratio to quench the reactions. Independent tests using a water-cooled probe were conducted to verify that the quartz probe effectively quenched the gas sample. The uncertainties of temperature and emissions measurements were calculated using the bias errors provided by manufacturer and the precision errors calculated by repeating experiments eight times. Concentrations are reported on an uncorrected, dry basis.

A three-way manual traversing system with least count of 0.6 mm was used to obtain temperature and emissions profiles within the combustor in radial $r$ and streamwise $Z$ directions. The downstream surface of the PIM was taken as the reference location ($Z = 0$ mm) for streamwise measurements. Experiments were conducted for two values of reactant flow velocities, $V_{\text{in}} = 0.5$ and 1.0 m/s. Here, the mean reactant velocity $V_{\text{in}}$ is calculated from the volume flow rate of the reactants (fuel and air) at ambient conditions divided by the cross-sectional area of the combustor chamber. The cold-flow Reynolds number based on the diameter of the combustion chamber was 670 and 1330 for the two cases. The heat release rates for the two cases were 230 W (0.7 MW/m$^2$) and 460 W (1.5 MW/m$^2$) at equivalence ratio $\Phi = 0.47$; here PIM surface area has been used to characterize the heat release rate, which is the typical approach used for surface burners.

## IV. Results and Discussion

Stable combustion was achieved on the surface of the inner PIM over a range of equivalence ratios for both reactant flow rates. Figure 3 shows preheat and product gas (at $r = 0$ mm and $Z = 63$ mm) temperatures during the warm-up period. After ignition, heat was transferred through the combustor wall by conduction

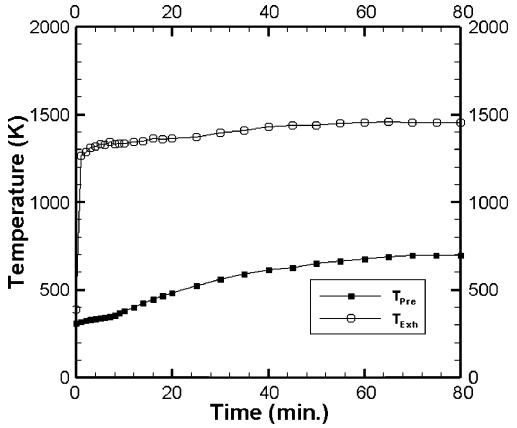


**Fig. 3 Transient nature of preheat and product gas temperatures during warm-up period.**

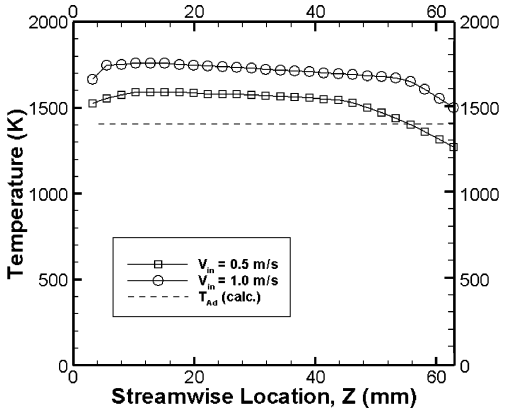


**Fig. 4 Streamwise temperature profile along the combustor centerline ($r = 0$ mm), $\Phi = 0.47$.**

and to the reactants by interfacial convection with PIM in the annulus. Increasing heat transfer to the reactants is evident by the increase in the preheat temperature $T_{pre}$ with time. Figure 3 shows that the product gas temperature $T_{exh}$ increased as the preheat temperature increased with time. The warm-up process took about 60 min to reach steady state for an insulated combustor with PIM in the annulus, $V_{in} = 1.0$ m/s and $\Phi = 0.47$. From practical considerations, future design would require a reduction in the thermal mass of the system to shorten the warm-up period.

### A. Effect of Reactant Flow Velocity

The product gas temperature in the streamwise direction at $r = 0$ mm is presented in Fig. 4. For $V_{in} = 1.0$ m/s, the temperature peaked within $Z = 10$ mm of the reaction zone. Figure 4 also shows the adiabatic flame temperature of the reactants at the annulus inlet, computed using the CHEMKIN equilibrium code.[22] The product gas temperature exceeded the adiabatic flame temperature because of the preheating of the reactants before combustion. A small drop in temperature in the region $10 < Z < 45$ mm indicates little heat transfer in the combustor midsection. The product gas temperature decreased sharply near the combustor exit. This is explained by the large temperature difference across the wall near the combustor exit plane, where the cooler reactants enter the annulus. Results indicate minimal effect on preheating if a shorter combustor was used. A similar trend was observed at the lower reactant flowrate with $V_{in} = 0.5$ m/s. However, the product gas temperature decreased by about 200 K, indicating that a greater fraction of heat released was lost to the surroundings. The heat release rate for $V_{in} = 1.0$ m/s is twice the heat release rate for $V_{in} = 0.5$ m/s. However, heat transfer through the combustor wall is not directly proportional to the heat release rate. Evidently, a greater fraction of heat released for the higher velocity case is retained in product gases, and a smaller fraction is lost to the surroundings.

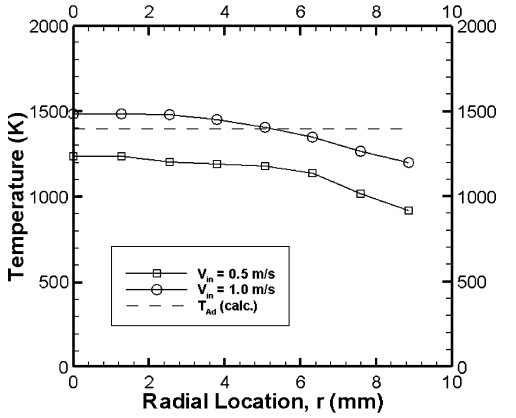


**Fig. 5 Radial temperature profile at combustor exit plane ($Z = 63$ mm), $\Phi = 0.47$.**

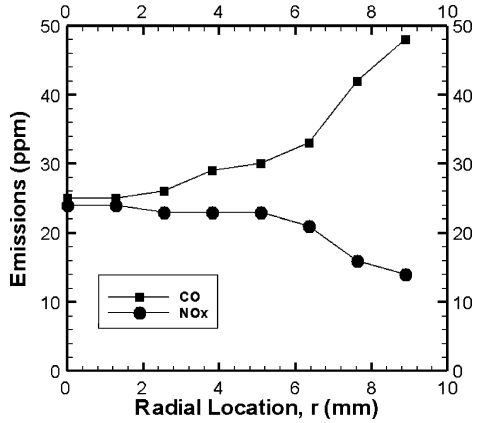


**Fig. 6 Radial profile of CO and NOx concentrations at $Z = 40$ mm, $\Phi = 0.47$, and $V_{in} = 1.0$ m/s.**

Figure 5 shows radial profiles of product gas temperature at the combustor exit plane, $Z = 63$ mm. For $V_{in} = 1.0$ m/s, the temperature at $r = 0$ mm is higher and that near the wall is lower than the adiabatic flame temperature of the reactants. Note that the bulk-averaged temperature at the combustor exit plane must be lower than the adiabatic flame temperature because of the heat loss to the surroundings. The temperature gradient near the combustor wall implies heat transfer through the combustor wall to preheat the reactants. The product gas temperature for $V_{in} = 0.5$ m/s was 200 K lower that that for $V_{in} = 1.0$ m/s.

Figure 6 presents CO and NOx concentration profiles in the radial direction taken at $Z = 40$ mm for $V_{in} = 1.0$ m/s. The CO concentration was the minimum at $r = 0$ mm and higher CO values were observed near the wall, where the temperature was lower, as seen in Fig. 5. Higher CO concentration is likely caused by incomplete oxidation near the combustor wall. Figure 6 shows that NOx concentration was highest at the center of the combustor and it decreased toward the wall. In this case, the cooler region near the wall has likely reduced the thermal NOx production. Note that the thermal NOx mechanism is important in this combustor even though the product gas temperatures below 1500 K at the combustor exit plane in Fig. 5 may suggest otherwise. This is because NOx emissions are produced in the reaction zone near the PIM, $Z < 10$ mm, where the flame temperature is 200–400 K higher than the temperature at the combustor exit plane.

Streamwise profiles of CO concentration along the combustor centerline are presented in Fig. 7. For $V_{in} = 1.0$ m/s, the CO concentration increased from a minimum of 22 ppm at $Z = 15$ mm to 30 ppm at the combustor exit. The gradual increase in CO concentration in the streamwise direction is attributed to the mixing of product gases as the flowfield in the combustion chamber developed downstream of the PIM. This explanation is supported by the increase in CO emissions in the radial direction, as seen in Fig. 6.

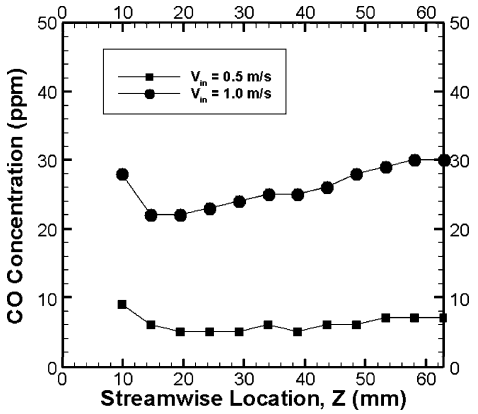


**Fig. 7 Streamwise CO concentration profile along combustor centerline ($r = 0$ mm), $\Phi = 0.47$.**

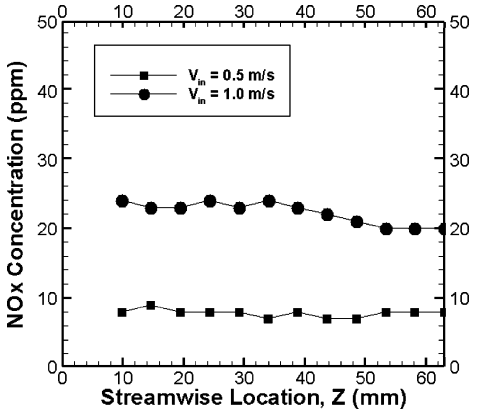


**Fig. 8 Streamwise NOx concentration profile along combustor centerline ($r = 0$ mm), $\Phi = 0.47$.**

The CO concentration for $V_{in} = 1.0$ m/s was significantly higher than that for the $V_{in} = 0.5$ m/s case. Even though the flame temperature is higher, increased CO emissions for the higher velocity case are likely caused by the shorter residence time in the reaction zone.

Streamwise profiles of NOx concentration along the combustor centerline are presented in Fig. 8. For $V_{in} = 1.0$ m/s, NOx emissions decreased from a maximum of 25 ppm at $Z = 10$ mm to 20 ppm at the combustor exit plane. The slight reduction in NOx concentration is attributed to mixing with products with lower NOx concentrations formed near the wall. NOx concentrations for $V_{in} = 0.5$ m/s were lower than those for $V_{in} = 1.0$ m/s, presumably because of the lower product gas temperature for the former case as seen in Fig. 4.

### B. Effect of Equivalence Ratio

The preheat temperature and product gas temperature at the centerpoint of the combustor exit plane, measured at various equivalence ratios, are presented in Fig. 9. Equivalence ratio was varied by adjusting both fuel and air flow rates, to maintain a constant reactant flow velocity. For $V_{in} = 1.0$ m/s, significant preheating occurred as indicated by $T_{pre}$ of 600–700 K. The product gas temperature at $r = 0$ mm exceeded the adiabatic flame temperature for all equivalence ratios. $T_{pre}$ increased slightly with increasing equivalence ratio, whereas the rise in $T_{exh}$ is more noticeable. For $V_{in} = 0.5$ m/s, the preheat temperature was approximately equal to that measured for $V_{in} = 1.0$ m/s. However, the product gas temperature for $V_{in} = 0.5$ m/s was lower by about 250 K, indicating greater fractional heat loss as discussed earlier. The LBO limit, represented by the data point with the smallest $\Phi$, was $\Phi = 0.39$ for $V_{in} = 0.5$ m/s and $\Phi = 0.41$ for $V_{in} = 1.0$ m/s. Because of the high level of preheating of the reactants, the LBO limit in the present system is significantly lower than the LBO limit of about $\Phi = 0.55$ in a typical swirl-stabilized combustor operating at similar conditions.

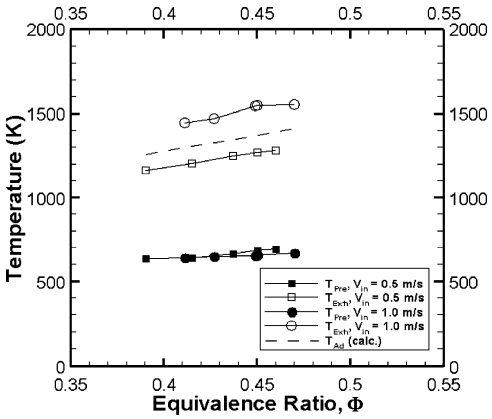


**Fig. 9 Effect of equivalence ratio on preheat and product gas temperatures.**

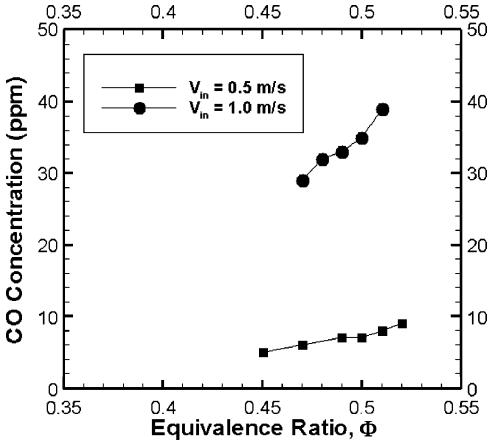


**Fig. 10 Effect of equivalence ratio on CO concentration at $r = 0$ mm and $Z = 63$ mm.**

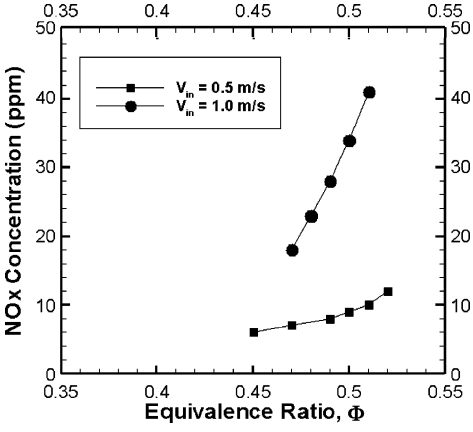


**Fig. 11 Effect of equivalence ratio on NOx concentration at $r = 0$ mm and $Z = 63$ mm.**

Figure 10 presents CO concentrations at $r = 0$ mm and $Z = 63$ mm for different equivalence ratios. The CO emissions increased with increasing equivalence ratio for both flow rates. The CO concentration was greater for the higher velocity case, which is consistent with Fig. 7. Figure 11 shows that the NOx concentrations at $r = 0$ mm and $Z = 63$ mm increased with equivalence ratio. Higher NOx values appear to correlate with higher product gas temperatures measured for the higher velocity case. The slope of NOx emission vs equivalence ratio curve is also greater for the higher velocity case with higher product gas temperatures as shown in Fig. 9.

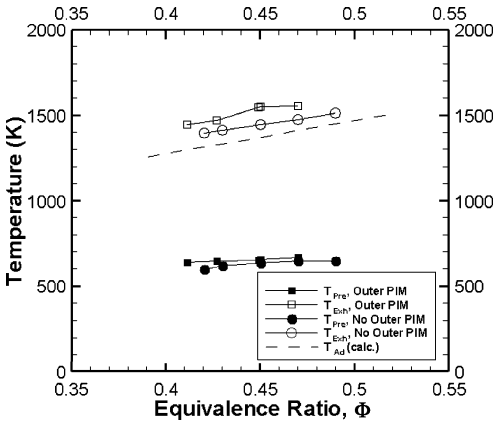


**Fig. 12 Preheat and product gas temperatures with and without PIM in the annulus.**

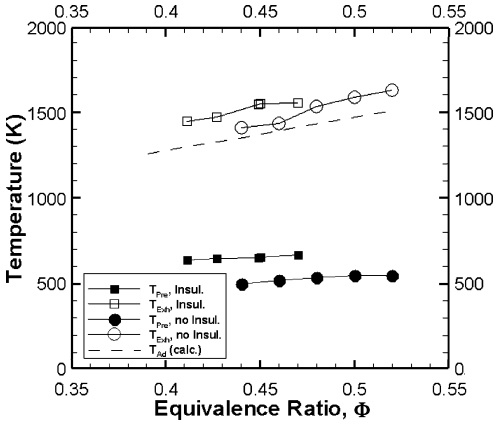


**Fig. 13 Preheat and product gas temperatures with and without surface insulation.**

### C. Effect of PIM in the Annulus

Experiments were performed to determine how PIM in the annulus effected heat recirculation and heat loss. PIM in the annulus is expected to increase heat recirculation and reduce heat loss by increasing the surface area for interfacial convection. Increased heat transfer to the exterior surface with the use of PIM in the annulus could also increase the heat loss. Figure 12 presents $T_{\text{pre}}$ and $T_{\text{exh}}$ for $V_{\text{in}} = 1.0$ m/s. Somewhat unexpectedly, the preheat temperature was nearly the same with and without PIM in the annulus, indicating that heat recirculation was not affected by PIM in the annulus. PIM in the annulus, however, resulted in slightly higher product gas temperatures, signifying a reduction in the heat loss. These results show that PIM in the annulus is effective in reducing combustor wall heat transfer. Several parameters including porosity, pore size, thermal conductivity, specific heat capacity, etc., affect the performance of PIM in the annulus. Detailed examination of these parameters, although useful, is beyond the scope of this study.

### D. Effect of Surface Insulation

Experiments were performed to determine the effect of insulating exterior surfaces of the system. Insulation is expected to improve thermal performance by reducing heat loss to the surroundings. Figure 13 presents $T_{\text{pre}}$ and $T_{\text{exh}}$ for $V_{\text{in}} = 1.0$ m/s. Insulation increased the preheat temperature by 150 K to reach a value of about 700 K. The LBO limit decreased from $\Phi = 0.44$ to $\Phi = 0.41$ with insulation. Accordingly, the product gas temperature was higher with insulation, indicating less heat loss.

### E. Energy Balance Calculations

Next, an energy balance based on control volume analysis was performed using experimental measurements to evaluate the thermal characteristics. Percent heat recirculation to the reactants in the annulus using the lower heating value (LHV) of the fuel was calculated as

$$\text{heat recirculation (\%)} = \frac{\dot{Q}_{\text{recirculation}}}{\dot{Q}_{\text{release}}} \cdot 100 = \frac{\sum_{\text{pre}} \dot{m} \cdot h - \sum_{\text{inlet}} \dot{m} \cdot h}{\dot{m}_f \cdot \text{LHV}} \cdot 100 \quad (1)$$

where $\dot{m}$ is the mass flow rate, $h$ is the total (chemical plus sensible) enthalpy, and $\dot{m}_f$ is the mass flow rate of the fuel. Subscripts inlet and pre represent summations taken, respectively, at the annulus inlet and preheat thermocouple location. Heat loss from the system to the surroundings was calculated as

$$\text{heat loss (\%)} = \frac{\dot{Q}_{\text{loss}}}{\dot{Q}_{\text{release}}} \cdot 100 = \frac{\sum_{\text{inlet}} \dot{m} \cdot h - \sum_{\text{outlet}} \dot{m} \cdot h}{\dot{m}_f \cdot \text{LHV}} \cdot 100 \quad (2)$$

where the summation at the outlet was obtained using measured product gas temperature profile (Fig. 5) and axial velocity (and mass flow rate) profile estimated from a computational fluid dynamic model.[23]

**Table 1 Heat generation, heat transfer, heat recirculation, and heat loss[a]**

| $V_{\text{in}}$, m/s | Heat release rate, W | PIM in preheat annulus | Exterior insulation | Combustor wall heat transfer, % | Heat recirculation, % (%) | Heat loss, % (%) |
|---|---|---|---|---|---|---|
| 0.5 | 230 | Yes | Yes | 63 | 32 (51) | 31 (49) |
| 1.0 | 460 | Yes | Yes | 37 | 30 (81) | 7 (19) |
| 1.0 | 460 | No | Yes | 43 | 28 (65) | 15 (35) |
| 1.0 | 460 | Yes | No | 34 | 17 (50) | 17 (50) |

[a] $\Phi = 0.47$ for all cases.

Table 1 presents combustor wall heat transfer, heat recirculation to the reactants, and heat loss to the surroundings calculated as percentage of heat released, also listed in the second column. Values calculated as percentages of combustor wall heat transfer are shown in parentheses. Note that the combustor wall heat transfer is the sum of the heat recirculation and heat loss. Results in Table 1 show that the combustor wall heat transfer decreased from 62 to 37% when the reactant velocity increased from $V_{\text{in}} = 0.5$ to 1.0 m/s. For $V_{\text{in}} = 0.5$ m/s, approximately one-half of the combustor wall heat transfer was recirculated to the reactants and the remaining one-half was lost to the surroundings. For $V_{\text{in}} = 1.0$ m/s, the heat loss decreased to about 20%, indicating more effective heat recirculation at higher heat release rates. This feature of the present design is important to develop miniature high-intensity combustion systems.

Table 1 shows that, in the absence of PIM in the annulus, the combustor wall heat transfer increased slightly from 37 to 43% and the heat loss to the surroundings increased from 7 to 15%. Accordingly, a smaller fraction of combustor wall heat transfer was recirculated to the reactants: 81% with PIM and 65% without PIM. These results show that PIM in the annulus was effective in reducing heat loss to the surroundings to improve heat recirculation to the reactants. Insulating the exterior surfaces had only a marginal effect on combustion wall heat transfer: 37% with insulation and 34% without insulation. However, insulation had a major effect on both heat loss and heat recirculation. With insulation a greater fraction of the combustor wall heat transfer was recirculated to the reactants (81% with insulation and 50% without insulation), and hence, a smaller fraction was lost to the surroundings.

## V. Conclusions

A heat-recirculating combustor using an annular preheating section is presented for mesoscale applications. The system performance was evaluated for methane fuel burning with air at ambient inlet conditions. Results show preheating of reactants to temperatures in excess of 600 K using thermal energy from the reaction zone. Preheating of the reactants allowed very lean combustion, with equivalence ratio of about 0.40 at LBO. The NOx and

CO concentrations increased with increasing the reactant flow rate. The maximum product gas temperature was higher than the adiabatic flame temperature of the reactants at inlet conditions. Heat loss to the surroundings as percentage of heat released in the combustor decreased at higher reactant flow rates (or higher heat release rates). Porous inert media in the preheating annulus and insulation on the exterior surfaces also reduced heat loss to the surroundings and improved preheating of the reactants. Results show that the present design offers potential to minimize the heat loss by achieving effective heat recirculation. Heat recirculation could be utilized to prevaporize liquid fuels, although only a gaseous fuel was investigated in this study. The overall system performance depends on several geometric parameters and material properties, which must be investigated in detail to develop optimal designs.

## Acknowledgments

This research was supported in part by the Graduate Assistance in Areas of National Need Program of the U.S. Department of Education and by the U.S. Army Research Laboratory and the U.S. Army Research Office under Grant DAAD 190210082.

## References

[1]Fernandez-Pello, A. C., "Micropower Generation Using Combustion: Issues and Approaches," *Proceedings of the Combustion Institute*, Vol. 29, The Combustion Inst., Pittsburgh, PA, 2002, pp. 883–889.

[2]Epstein, A. H., "Millimeter-Scale, MEMS Gas Turbine Engines," American Society of Mechanical Engineers, ASME Paper GT-2003-38866, June 2003.

[3]Yuasa, S., Oshimi, K., Nose, H., and Tennichi, Y., "Concept and Combustion Characteristics of Ultra-Micro Combustors with Premixed Flame," *Proceedings of the Combustion Institute*, Vol. 30, The Combustion Inst., Pittsburgh, PA, 2005, pp. 2455–2462.

[4]Norton, D. G., and Vlachos, D. G., "Hydrogen Assisted Self-Ignition of Propane/Air Mixtures in Catalytic Microburners," *Proceedings of the Combustion Institute*, Vol. 30, The Combustion Inst., Pittsburgh, PA, 2005, pp. 2473–2480.

[5]Boyarko, G. A., Sung, C.-J., and Schneider, S. J., "Catalyzed Combustion of Hydrogen–Oxygen in Platinum Tubes for Micro Propulsion Applications," *Proceedings of the Combustion Institute*, Vol. 30, The Combustion Inst., Pittsburgh, PA, 2005, pp. 2481–2488.

[6]Ju, Y., and Xu, B., "Theoretical and Experimental Studies on Mesoscale Flame Propagation and Extinction," *Proceedings of the Combustion Institute*, Vol. 30, The Combustion Inst., Pittsburgh, PA, 2005, pp. 2445–2454.

[7]Kyritsis, D. C., Roychoudhury, S., McEnally, C. S., Pfefferle, L. D., and Gomez, A., "Mesoscale Combustion: A First Step Towards Liquid Fueled Batteries," *Experimental Thermal and Fluid Science*, Vol. 28, No. 7, 2004, pp. 97–104.

[8]Lee, D. H., and Kwon, S., "Scale Effects on Combustion Phenomena in a Microcombustor," *Microscale Thermophysical Engineering*, Vol. 7, No. 3, 2003, pp. 235–251.

[9]Waitz, I. A., Gauba, G., and Tzeng, Y. S., "Combustors for Micro-Gas Turbine Engines," *Journal of Fluids Engineering*, Vol. 120, March 1998, pp. 109–117.

[10]Leach, T. T., and Cadou, C. P., "The Role of Structural Heat Exchange and Heat Loss in the Design of Efficient Silicon Micro-Combustors," *Proceedings of the Combustion Institute*, Vol. 30, The Combustion Inst., Pittsburgh, PA, 2005, pp. 2437–2444.

[11]Hardesty, D. R., and Weinberg, F. J., "Burners Producing Large Excess Enthalpies," *Combustion Science and Technology*, Vol. 8, No. 4, 1974, pp. 201–214.

[12]Ahn, J., Eastwood, C., Sitzki, L., and Ronney, P., "Gas Phase and Catalytic Combustion in Heat Recirculating Burners," *Proceedings of the Combustion Institute*, Vol. 30, The Combustion Inst., Pittsburgh, PA, 2005, pp. 2463–2472.

[13]Ronney, P. D., "Analysis of Non-Adiabatic Heat Recirculating Combustors," *Combustion and Flame*, Vol. 135, No. 4, 2003, pp. 421–439.

[14]Sirignano, W. A., Pham, T. K., and Dunn-Rankin, D., "Miniature-Scale Liquid-Fuel-Film Combustor," *Proceedings of the Combustion Institute*, Vol. 29, The Combustion Inst., Pittsburgh, PA, 2002, pp. 925–931.

[15]Yetter, R. A., Yang, V., Wang, Z., Wang, Y., Milius, D. L., Peluse, M. J., Aksay, I. A., Angioletti, M., and Dryer, F. L., "Development of Meso and Micro Scale Liquid Propellant Thrusters," AIAA Paper 2003-0676, Jan. 2003.

[16]Takeno, T., and Sato, K., "An Excess Enthalpy Flame Theory," *Combustion Science and Technology*, Vol. 20, No. 1, 1979, pp. 70–84.

[17]Trimis, D., and Durst, F., "Combustion in a Porous Medium—Advances and Applications," *Combustion Science and Technology*, Vol. 121, No. 2, 1996, pp. 153–168.

[18]Howell, J. R., Hall, M. J., and Ellzey, J. L., "Radiation Enhanced/Controlled Phenomena of Heat and Mass Transfer in Porous Media," *Progress in Energy and Combustion Science*, Vol. 22, No. 2, 1996, pp. 121–145.

[19]Marbach, T. L., and Agrawal, A. K., "Experimental Study of Surface and Interior Combustion Using Composite Porous Inert Media," *Journal of Engineering for Gas Turbines and Power*, Vol. 127, No. 2, 2005, pp. 307–313.

[20]Marbach, T. L., and Agrawal, A. K., "Fuel Vaporization and Combustion with the Use of Porous Inert Media," AIAA Paper 2003-5090, July 2003.

[21]Insulfrax website, Unifrax Corporation, http://www.insulfrax.com [cited June 2002].

[22]Kee, R. J., Rupley, F. M., and Miller, J. A., "Chemkin-II: A FORTRAN Chemical Kinetics Package for the Analysis of Gas Phase Chemical Kinetics," Sandia National Labs., Rept. SAND89-809B-UC-706, Albuquerque, NM, May 1989.

[23]Marbach, T. L., and Agrawal, A. K., "Experimental and Numerical Study of a Heat Recirculating Combustion for Meso-Scale Application," *4th Joint Meeting of the U.S. Sections of the Combustion Institute*, Paper D01, March 2005.